




Use of Synthetic Hybrid Strains To Determine the Role of Replicon 3 in Virulence of the *Burkholderia cepacia* Complex

 Kirsty Agnoli,^a Roman Freitag,^{a*} Margarida C. Gomes,^b Christian Jenul,^a Angela Suppiger,^a Olga Mannweiler,^a Carmen Frauenknecht,^{a*} Daniel Janser,^a Annette C. Vergunst,^b Leo Eberl^a

Department of Plant and Microbial Biology, University of Zürich, Zürich, Switzerland^a; VBMI, INSERM, Université de Montpellier, Nîmes, France^b

ABSTRACT The *Burkholderia cepacia* complex (Bcc) displays a wealth of metabolic diversity with great biotechnological potential, but the utilization of these bacteria is limited by their opportunistic pathogenicity to humans. The third replicon of the Bcc, megaplasmid pC3 (0.5 to 1.4 Mb, previously chromosome 3), is important for various phenotypes, including virulence, antifungal, and proteolytic activities and the utilization of certain substrates. Approximately half of plasmid pC3 is well conserved throughout sequenced Bcc members, while the other half is not. To better locate the regions responsible for the key phenotypes, pC3 mutant derivatives of *Burkholderia cenocepacia* H111 carrying large deletions (up to 0.58 Mb) were constructed with the aid of the FLP-FRT (FRT, flippase recognition target) recombination system from *Saccharomyces cerevisiae*. The conserved region was shown to confer near-full virulence in both *Caenorhabditis elegans* and *Galleria mellonella* infection models. Antifungal activity was unexpectedly independent of the part of pC3 bearing a previously identified antifungal gene cluster, while proteolytic activity was dependent on the nonconserved part of pC3, which encodes the ZmpA protease. To investigate to what degree pC3-encoded functions are dependent on chromosomally encoded functions, we transferred pC3 from *Burkholderia cenocepacia* K56-2 and *Burkholderia lata* 383 into other pC3-cured Bcc members. We found that although pC3 is highly important for virulence, it was the genetic background of the recipient that determined the pathogenicity level of the hybrid strain. Furthermore, we found that important phenotypes, such as antifungal activity, proteolytic activity, and some substrate utilization capabilities, can be transferred between Bcc members using pC3.

IMPORTANCE The *Burkholderia cepacia* complex (Bcc) is a group of closely related bacteria with great biotechnological potential. Some strains produce potent antifungal compounds and can promote plant growth or degrade environmental pollutants. However, their agricultural potential is limited by their opportunistic pathogenicity, particularly for cystic fibrosis patients. Despite much study, their virulence remains poorly understood. The third replicon, pC3, which is present in all Bcc isolates and is important for pathogenicity, stress resistance, and the production of antifungal compounds, has recently been reclassified from a chromosome to a megaplasmid. In this study, we identified regions on pC3 important for virulence and antifungal activity and investigated the role of the chromosomal background for the function of pC3 by exchanging the megaplasmid between different Bcc members. Our results may open a new avenue for the construction of antifungal but nonpathogenic *Burkholderia* hybrids. Such strains may have great potential as biocontrol strains for protecting fungus-borne diseases of plant crops.

Received 24 February 2017 Accepted 12 April 2017

Accepted manuscript posted online 21 April 2017

Citation Agnoli K, Freitag R, Gomes MC, Jenul C, Suppiger A, Mannweiler O, Frauenknecht C, Janser D, Vergunst AC, Eberl L. 2017. Use of synthetic hybrid strains to determine the role of replicon 3 in virulence of the *Burkholderia cepacia* complex. *Appl Environ Microbiol* 83:e00461-17. <https://doi.org/10.1128/AEM.00461-17>.

Editor Marie A. Elliot, McMaster University

Copyright © 2017 American Society for Microbiology. All Rights Reserved.

Address correspondence to Kirsty Agnoli, kagnoli@botinst.uzh.ch, or Leo Eberl, leberl@botinst.uzh.ch.

* Present address: Roman Freitag, Hays (Schweiz) AG, Zürich, Switzerland; Carmen Frauenknecht, Institut für Rechtsmedizin, Kantonsspital Aarau, Switzerland.

KEYWORDS *Burkholderia*, *Caenorhabditis elegans*, antifungal agents, multiple replicons, synthetic biology, virulence

The *Burkholderia cepacia* complex (Bcc) is a group of closely related species of the genus *Burkholderia*, currently numbering 21 species (1–4). The complex is of both medical and biotechnological importance, medical because of the strains' ability to cause infections in cystic fibrosis and immunocompromised patients, and biotechnological due to their plant growth-promoting and biocontrol capabilities (5). The environment is known to be a source of Bcc acquisition (6, 7), which has prevented the realization of the agricultural potential of these bacteria (8). The Bcc genome is large (nearly 8 Mb for *Burkholderia cenocepacia* H111) and consists of at least three replicons; these are chromosomes 1 and 2 and the megaplasmid pC3. pC3 was previously known as chromosome 3 but has been found to be nonessential in every Bcc strain investigated so far (9, 10). The large Bcc genome size and multireplicon structure enable Bcc strains to thrive in a range of different niches, both agricultural and medical. This division is a typical feature of other members of the *Burkholderia* genus, where the primary chromosome specifies the majority of the core genome, and more specialist lifestyle-determining genes are present on the secondary replicons (11). For example, in *Burkholderia xenovorans* LB400, chromate resistance and degradation of the environmental pollutant polychlorinated biphenyl (PCB) are specified by its megaplasmid, which appears to be a patchwork of genes acquired from various other bacteria (11, 12). Genomic comparisons of the *B. xenovorans* LB400 genome with other *Burkholderia* genomes suggested that its secondary replicons show increased sequence evolution rates compared to that of the primary chromosome (11). In addition to this, the secondary replicons of *Sinorhizobium meliloti* have been shown to have greater importance in the rhizosphere than in bulk soil (13). The multireplicon structure of the *Burkholderia* genus allows conservation of the core functions on a largely inviolate primary chromosome but with a high degree of acquisition of genetic material on secondary replicons, resulting in great adaptability (13–15).

The primary chromosome is highly conserved among Bcc strains and encompasses the majority of the core genome (14). The less-conserved secondary chromosome contains genes important for niche adaptation of individual Bcc strains, whereas megaplasmid pC3 has roles in virulence and antifungal activity in various Bcc species, which are, to various degrees, dependent on the strain (9, 10). It has also been shown to be important for stress tolerance in *B. cenocepacia* H111 (10). A number of well-characterized genes and clusters contributing to these phenotypes are carried by pC3. For example, in terms of antifungal activity, the occidiofungin, *haq*, and enacyloxin genes are located on pC3 from *Burkholderia ambifaria* AMMD. The pyrrolnitrin genes *prnABCD* are located on pC3 from *B. lata* 383 (pC3₃₈₃), and the *afc* cluster is present on pC3 in several Bcc strains, including *B. cenocepacia* H111, where it is currently the only pC3-carried antifungal factor identified (16–20). Few pC3-carried genes associated with virulence have been identified, and those that have been constitute virulence factors in only a subset of model organisms. Those identified to date consist of a protease-encoding gene (*zmpA*) (21), the nematocidal gene *aidA* (22), and the lysR-type transcriptional regulator *shvR*, which regulates a number of phenotypes, including pathogenicity and the antifungal gene cluster *afc* (23, 24). ZmpA and ShvR have been shown to be important in *B. cenocepacia* K56-2 virulence against the rat but not to the lower organisms *Galleria mellonella* and *Caenorhabditis elegans*. Of the organisms tested, AidA appears to act as a virulence factor only against nematodes (25). This study aimed to localize the regions of pC3 conferring pathogenicity to H111 and to determine antifungal activity (as a phenotype relevant to biocontrol) and proteolytic activity (a virulence factor in higher organisms), through the construction and analysis of partial derivatives. Furthermore, we investigated how these phenotypic traits could be transferred when pC3s were swapped between different *B. cenocepacia* strains of clinical and environmental origin, and even between *B. cenocepacia* and *B. lata*. We aim eventually

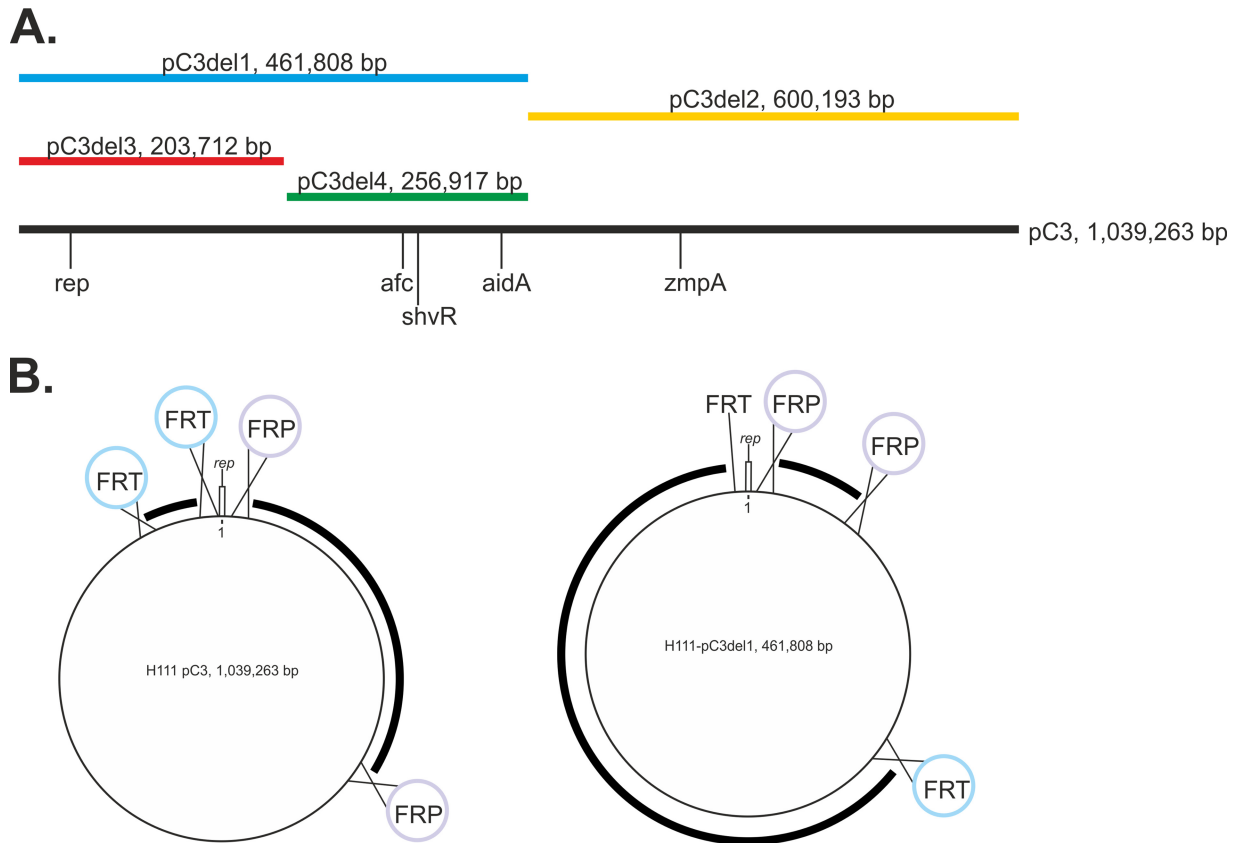


FIG 1 Organization and construction of pC3 partial derivatives. (A) pC3 region present in each derivative. In addition to the region shown, pC3del2 and pC3del4 also contained the region necessary for pC3 replication (*rep*). The regions present in pC3del1, pC3del2, pC3del3, and pC3del4 are shown in blue, yellow, red, and green, respectively. Key genes and regions (*afc* cluster, *shvR*, *aidA*, and *zmpA*) are indicated. (B) Positioning of *FRT* sites on pC3 for the construction of pC3del2 and pC3del4. Plasmid integrations were carried out sequentially, i.e., after positioning of the *FRT* sites, flipase-induced recombination was carried out to excise the intervening region, followed by integration of the *FRP*-bearing plasmids. Hence, all four sites were not present on pC3 at any point. The regions excised have been indicated using a heavy black line. Left subpanel, pC3del2 construction; right subpanel, pC3del4 construction.

to construct a tool kit for replicon shuffling within the Bcc, consisting of a nonvirulent chassis strain lacking pC3 and bearing a pared-down chromosome 2, into which we can introduce appropriately streamlined pC3s conferring phenotypes for different applications. Here, we use this technology as a first step to better understand the role of pC3 in virulence and antifungal activity.

RESULTS

Use of partial derivatives of pC3 to locate phenotypic traits. We have previously shown that pC3 is important for virulence, antifungal activity, and proteolytic activity in *B. cenocepacia* H111 (4). In order to locate the regions of pC3 responsible for these phenotypes, with an emphasis on virulence, we constructed a series of four partial derivatives of pC3_{H111}. We used an FLP-*FRT*-based (*FRT*, FLP recombination target) recombination strategy to construct deletion derivatives containing the pC3 origin of replication and part of pC3, as depicted in Fig. 1. We had previously determined that pC3_{H111} consists of two parts, one bearing genes highly conserved among the Bcc, and one bearing few such genes (9). Two derivatives were therefore constructed, one bearing the conserved part and one bearing the nonconserved part (pC3del1 and pC3del2, respectively). Two further pC3 derivatives were constructed, each bearing one half of the conserved region (pC3del3 and pC3del4). H111Δc3 strains bearing the partial pC3 derivatives were examined by a pathogenicity assay in *C. elegans* and *G. mellonella*, and by proteolytic and antifungal activity assays.

Proteolytic activity can be localized to the nonconserved part of H111 pC3. Analysis of the partial pC3 derivatives of H111 by an azocasein assay indicated that the

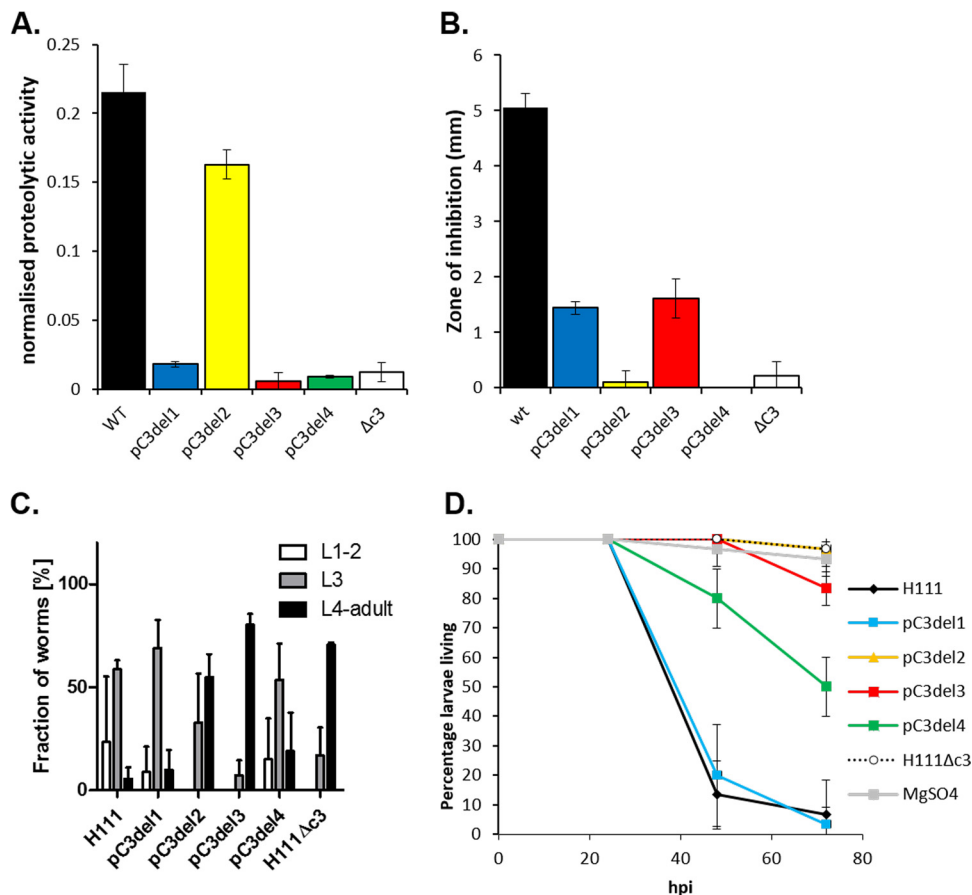


FIG 2 Phenotypes exhibited by H111 bearing partial pC3 derivatives. Control strains were H111 (wt) and an H111 pC3-null derivative ($\Delta c3$). The partial pC3 derivative present in each strain has been indicated. Error bars represent standard deviations of the results across biological triplicates, unless otherwise stated. (A) Proteolytic activity. Bars represent the normalized proteolytic activity of each strain at 37°C. (B) Antifungal activity against *F. solani*. Bars represent the mean zone of inhibition surrounding the bacteria. Plates were incubated at room temperature for 9 days. (C) Derivative pC3del4 confers full pathogenicity against nematodes. The percentage of nematodes within developmental stages L1 to -2, L3, and L4 to adult were assessed after 48 h of growth in liquid cultures of H111 bearing the partial pC3 derivatives indicated. Bars represent the means of two independent experiments, and error bars show the standard deviation. (D) Pathogenicity against *G. mellonella* requires the conserved region of pC3. Survival curves are for *G. mellonella* larvae infected with the H111 derivatives indicated. Larvae were injected with approximately 7.5×10^4 bacteria and incubated at 30°C in the dark. Live and dead larvae were counted at 24, 48, and 72 hpi. Significance was determined where pertinent using the log rank test; H111/pC3del3 did not differ significantly from H111 $\Delta c3$ ($P = 0.0878$).

gene or genes responsible for proteolytic activity are located on pC3del2 (Fig. 2). This derivative bears the region of pC3 that is poorly conserved in the Bcc. The construct includes the *zmpA* gene, which encodes a metalloprotease known to have activity on casein (9, 26). Furthermore, three other putative protease-encoding genes have been annotated on this part of pC3 (I35_7576, I35_7645, and I35_7805), whereas none have been annotated on the more conserved part. A conditional mutant bearing the *zmpA* gene under the control of a rhamnase-inducible promoter (H111-*zmpA*) showed an ~4-fold reduction in proteolytic activity relative to the wild type, compared to the ~5-fold reduction observed in the pC3-null mutant (Fig. 3B), showing that ZmpA contributes the major protease activity in this strain.

Antifungal activity is dependent on the conserved part of pC3. It was previously shown that pC3 is important for the antifungal activity of H111 and other Bcc members. This was found to be particularly clear when investigated by a dual-culture assay against *Fusarium solani* (9). None of the partial pC3 derivatives conferred full antifungal activity upon H111 (Fig. 2). Strains bearing the derivatives pC3del2 and pC3del4 had a level of antifungal activity similar to that of H111 $\Delta c3$, while strains bearing the partial

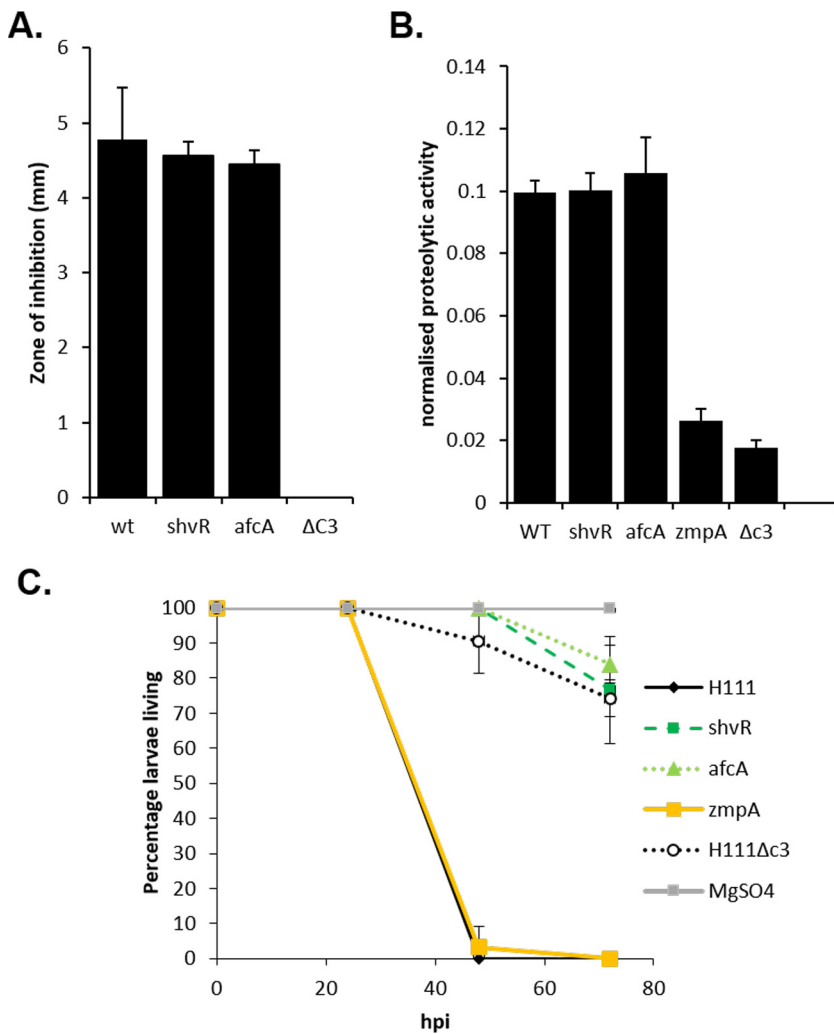


FIG 3 Phenotypes exhibited by H111-targeted gene mutants. Control strains were H111 (wt) and an H111 pC3-null derivative ($\Delta c3$). The gene targeted in each mutant is indicated. Error bars represent standard deviations of the results across biological triplicates. (A) *shvR* and *afcA* are dispensable for antifungal activity against *F. solani*. Bars represent the mean zone of inhibition surrounding the bacteria. Plates were incubated at room temperature for 9 days. (B) *zmpA* is important for proteolytic activity. Bars represent the normalized proteolytic activity of each strain at 37°C. (C) *shvR* and *afcA* are important for pathogenicity against *G. mellonella*. Survival curves are for *G. mellonella* larvae infected with H111 bearing the targeted mutations indicated. Larvae were injected with approximately 7.5×10^4 bacteria and incubated at 30°C in the dark. Live and dead larvae were counted at 24, 48, and 72 hpi.

derivatives pC3del1 and pC3del3 each showed a similar modest level of antifungal activity. In agreement with these data, antifungal activity remained unchanged in H111 after removal of the antifungal cluster *afc* and its regulator *shvR*, both located on pC3del4 (Fig. 3). This suggests that unknown functions encoded on the region present in pC3del3 have an important contribution to the full antifungal activity of this strain toward *F. solani*, and that the *afc* operon has no role in antifungal activity of H111 against *F. solani*, in contrast to what has been described for the virulence of *B. cenocepacia* K56-2 (23).

Conserved part of H111 pC3 is necessary for pathogenicity. Pathogenicity analysis of H111 $\Delta c3$ harboring the partial pC3 derivatives against *C. elegans* indicated that the part of pC3 present in pC3del4 was sufficient for full pathogenicity against this model organism (Fig. 2). This part of pC3 carries *aidA*, which is known to encode an important virulence factor for the pathogenicity of H111 to the nematode (22).

Pathogenicity assays using larvae of the greater wax moth (*G. mellonella*) as infection hosts (Fig. 2) showed that H111 containing the nonconserved part of pC3 (pC3del2)

showed no significant virulence in this model up to 76 hours postinfection (hpi) (Fig. 2D). Indeed, specific disruption of the *zmpA* gene carried in this region did not affect virulence to *G. mellonella* (Fig. 3B), in agreement with the findings in a previous work (27). However, the strain bearing pC3del1, which carries the conserved half of pC3, showed close-to-wild-type levels of pathogenicity. The strain bearing pC3del4, carrying the *shvR* and *afc* genes, conferred an intermediate level of virulence compared to that of pC3del1, but the strain bearing pC3del3 did not show similar virulence to H111Δc3. This suggests that virulence traits encoded by pC3del4 require additional virulence-related factors located on pC3del3 to obtain full pathogenicity. Mutations of *afcA* and *shvR*, both of which are carried by pC3del4 (Fig. 3C), indeed strongly attenuated pathogenicity, showing that these factors are important for the virulence of H111 to *G. mellonella*.

Replicon shuffling with pC3. Phylogenetic analyses suggest that pC3 was acquired vertically (9, 28), and we have previously shown that pC3 derivatives bearing an origin of transfer (*oriT*) can be mobilized by conjugation. This approach was successfully used to transfer pC3 from *B. cenocepacia* K56-2 to *B. cenocepacia* H111 lacking pC3 (10). To further investigate the different phenotypes encoded by pC3 and to elucidate any involvement of chromosomally encoded functions, we began a series of such transfers, both between *B. cenocepacia* strains differing in properties such as pathogenicity and between different species of interest within the Bcc. While all transfers attempted within *B. cenocepacia* were successful, namely, the transfer of pC3_{K56-2} into HI2424Δc3 and MCO3Δc3 (and H111Δc3, as described previously [10]), only two interspecies transfers were achieved, namely, pC3₃₈₃ of *B. lata* 383 into *B. cenocepacia* H111Δc3 and of pC3 of *B. cenocepacia* K56-2 (pC3_{K56-2}) into *B. lata* 383Δc3. The causes behind the observed limitations to free transfer of pC3 between Bcc species are under investigation.

pC3 transfer can confer virulence, depending on the strain background. The virulence of *B. cenocepacia* HI2424, MCO-3, and *B. lata* bearing pC3_{K56-2} instead of their native pC3 replicons was assessed in the zebrafish model of infection (Fig. 4). The virulence of H111 showed large variations between experiments and was therefore not further analyzed in this study.

We have previously shown that *B. cenocepacia* K56-2 (which is highly virulent for zebrafish embryos) and HI2424 (which shows intermediate virulence levels) did not cause fatal infection within 5 days (the time span of the experiments) in the absence of pC3 (9, 10). Transfer of pC3_{K56-2} into HI2424Δc3 significantly increased the mortality rate caused by the recipient strain, sometimes even to the level of the pC3 donor strain K56-2 (Fig. 4). Introduction of pC3_{K56-2} into the MCO-3 background restored full virulence of the recipient but did not increase virulence to the level of the more-pathogenic pC3 donor strain K56-2. In contrast, pC3_{K56-2} did not restore virulence to *B. lata* 383Δc3.

The same trend was also observed for these strains in the *C. elegans* model (Fig. 5). In addition, in this infection model, we also tested derivatives of *B. cenocepacia* H111Δc3 harboring pC3_{K56-2} or pC3₃₈₃. As for MCO-3 harboring pC3_{K56-2}, we observed that the virulence of the hybrid strains increased approximately to the level of the H111 wild-type strain but did not reach the virulence levels of the donor strains. In the *G. mellonella* model, the pC3-deleted *B. lata* 383 strain was not significantly reduced in virulence compared to the wild type and was indistinguishable from that of the donor strain K56-2 (Fig. 6). For the *B. cenocepacia* HI2424 and MCO-3 strain backgrounds, the survival curves of the hybrid strains were similar to those of the wild-type recipients and the K56-2 donor. Interestingly, the introduction of pC3_{K56-2} or pC3₃₈₃ into H111Δc3 gave rise to an intermediate level of virulence compared to that of the H111 parent strain.

Proteolytic activity can be conferred by pC3 transfer. Proteolytic activity was analyzed by the quantitative azocasein assay. All wild-type strains tested (*B. cenocepacia* MCO-3, HI2424, and H111, and *B. lata* 383) exhibited proteolytic activity (Fig. 7A and B).

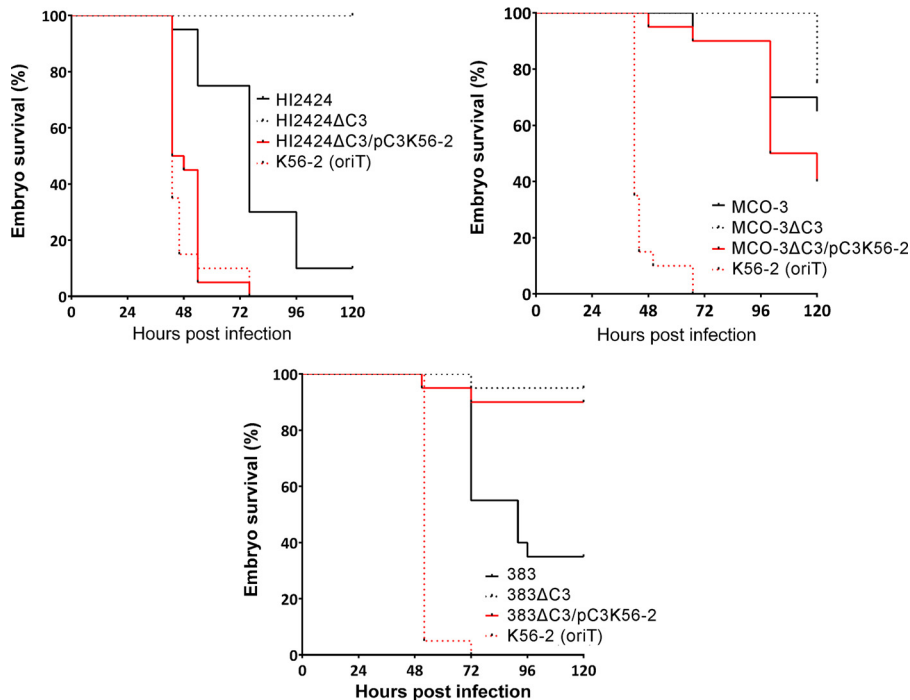


FIG 4 Virulence can be restored to wt levels in a pC3-null mutant by introduction of a nonnative pC3. Kaplan-Meier survival curves are for zebrafish embryos injected with the indicated strains. Embryos were incubated at 28°C. Dead embryos were scored at different time points after injection by absence of a heartbeat. Graphs are representative of the results from at least 3 independent experiments ($n = 20$ per group). Average inocula in the presented experiments: HI2424, 84 CFU; HI2424ΔC3, 164 CFU; HI2424/pC3_{K56-2}, 121 CFU; K56-2, 220 CFU; MCO-3, 104 CFU; MCO-3ΔC3, 91 CFU; MCO-3/pC3_{K56-2}, 159 CFU; K56-2, 151 CFU; 383, 55 CFU; 383ΔC3, 53 CFU; 383ΔC3/pC3_{K56-2}, 23 CFU; K56-2, 296 CFU. Significance was determined using the log rank test: HI2424ΔC3 versus HI2424, $P < 0.0001$; HI2424ΔC3/pC3_{K56-2} versus HI2424, $P < 0.0001$; HI2424ΔC3/pC3_{K56-2} versus K56-2, $P = 0.2315$; MCO-3ΔC3 versus MCO-3, $P = 0.3141$; MCO-3ΔC3/pC3_{K56-2} versus MCO-3, $P = 0.1462$; MCO-3ΔC3/pC3_{K56-2} versus K56-2, $P < 0.0001$; 383ΔC3 versus 383, $P < 0.0001$; 383ΔC3/pC3_{K56-2} versus 383, $P = 0.0006$; and 383ΔC3/pC3_{K56-2} versus K56-2, $P < 0.0001$.

For each strain background, the pC3-null derivative showed greatly reduced proteolytic activity. The introduction of pC3_{K56-2} into the pC3-null derivatives in each case conferred proteolytic activity (Fig. 7A and B). The levels of activity observed upon transfer of pC3_{K56-2} were higher than that of the donor strain from which this pC3 was transferred (indicated as K56-2 [oriT] in Fig. 7A and B). The introduction of pC3₃₈₃ (from *B. lata* 383) into H111Δc3 also resulted in proteolytic activity (Fig. 7B).

Antifungal activity can be conferred by introduction of a nonnative pC3. The antifungal activities of hybrid strains were assessed by a dual-culture assay against *F. solani* (Fig. 7C). The exchange of its native pC3 for pC3_{K56-2} conferred antifungal activity to *B. cenocepacia* MCO-3, which normally shows no such activity against *F. solani* (9). In *B. lata* 383 and *B. cenocepacia* H111, which showed no antifungal activity against the fungus in the absence of pC3, the introduction of pC3_{K56-2} fully restored antifungal activity. Likewise, while HI2424ΔC3 showed reduced antifungal activity relative to HI2424, the introduction of pC3_{K56-2} increased the activity of the strain almost to the level of the wild type. Interestingly, the introduction of pC3₃₈₃ into H111Δc3 restored the antifungal activity of the strain only to the level of the pC3 donor strain *B. lata* 383.

Transferring pC3 results in the mingling of metabolic phenotypes. Phenotypic microarrays were carried out to analyze carbon and nitrogen source utilization by H111 bearing pC3_{K56-2} or pC3₃₈₃. Utilization phenotypes were compared with the parent strain (H111Δc3), the pC3 donor strain, and the wild-type H111 strain, and for the pC3₃₈₃ transfer, *B. lata* 383Δc3. Phenotypic differences showing a >2-fold growth increase between strains being compared were considered. The deletion of pC3 from H111 results in the loss of nine carbon and four nitrogen utilization phenotypes (9). The

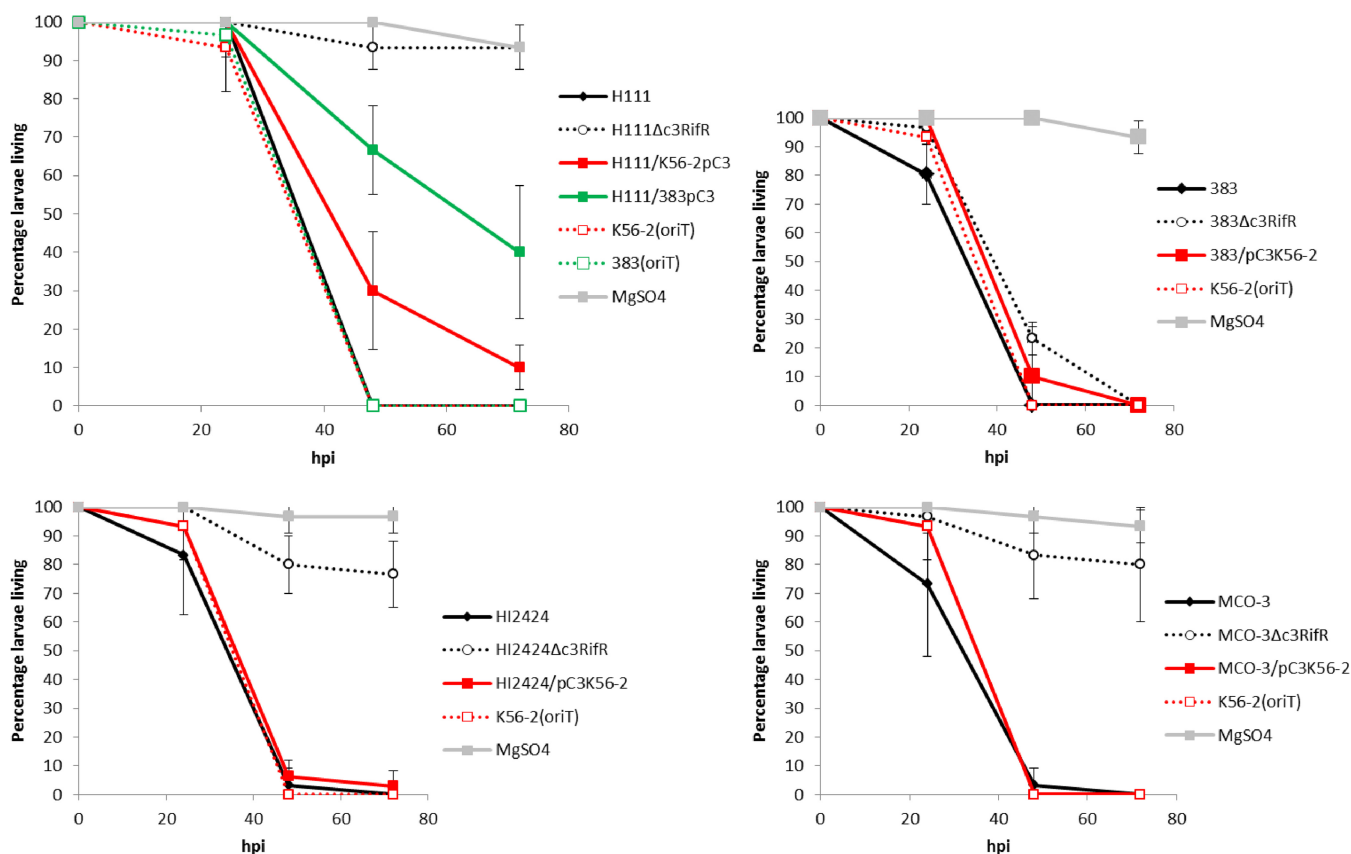


FIG 5 Virulence against *C. elegans* can be restored to wt levels in a pC3-null mutant by introduction of a nonnative pC3. The percentage of nematodes within developmental stages L1 to -2, L3, and L4 to adult were assessed after 48 h of growth in liquid cultures of the strains indicated. Bars represent the means of the results from two independent experiments, and error bars show the standard deviation.

transfer of pC3 of *B. lata* (pC3₃₈₃) into H111Δc3 rescued two carbon and two nitrogen utilization phenotypes (carbon sources, caproic acid and butyric acid; nitrogen sources, histamine and D-galactosamine). Additionally, H111Δc3/pC3₃₈₃ was able to utilize *m*-tartaric acid as a carbon source, a phenotype not present in either H111Δc3 or H111. *B. lata* 383 is able to utilize *m*-tartaric acid as a carbon source, and this phenotype is dependent on pC3 (9). Transfer of pC3_{K56-2} into H111Δc3 rescued five carbon utilization phenotypes and one nitrogen utilization phenotype (carbon sources, D-xylose, gelatin, caproic acid, citraconic acid, and putrescine; nitrogen source, histamine). Additionally, H111Δc3/pC3_{K56-2} was able to utilize tricarballic acid as a carbon source, a phenotype not present in either H111Δc3 or H111. *B. cenocepacia* K56-2 is able to utilize tricarballic acid as a carbon source, and this phenotype is dependent on pC3 (Table 1). Interestingly, the introduction of pC3₃₈₃ into H111Δc3 resulted in the loss of three carbon (L-fucose, *m*-hydroxyphenylacetic acid, and D-arabinose) and three nitrogen (agmatine, xanthosine, and L-homoserine) utilization phenotypes, and the introduction of pC3_{K56-2} into H111Δc3 resulted in the loss of six nitrogen utilization phenotypes (L-homoserine, agmatine, guanine, adenosine, acetamide, and D,L-lactamide).

DISCUSSION

Partial derivative pC3del4 conferred virulence but not proteolytic or antifungal activity upon H111Δc3. Antifungal activity in the Bcc has been shown to be pC3 dependent (9, 10). *B. cenocepacia* H111 exhibits potent activity against *F. solani*, whereas a pC3-null mutant shows no such activity. It was previously reported that this strain carries the *afc* cluster on pC3, and this was thought to be responsible for its pC3-dependent antifungal activity (9). The *afc* cluster is located in the part of pC3 present in the pC3del4 derivative constructed during this study, as is the *shvR* gene,

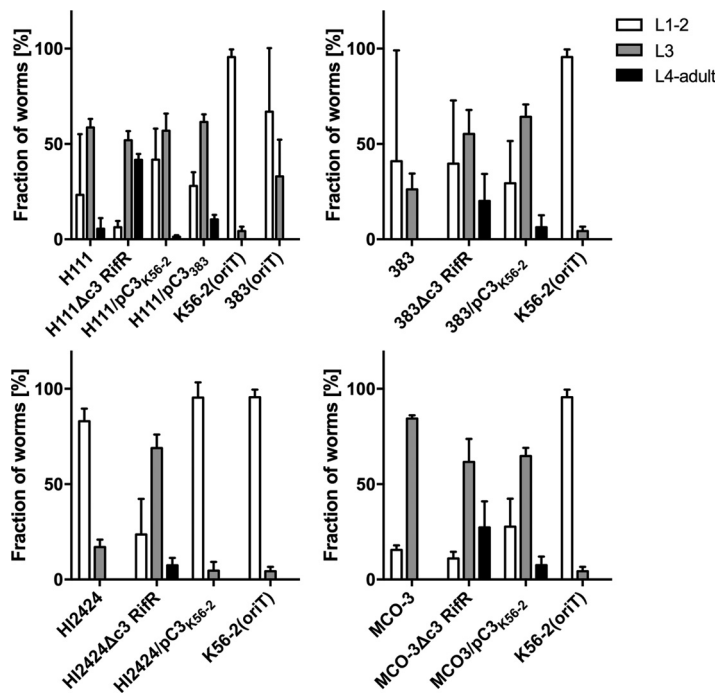


FIG 6 Nonnative pC3s can confer virulence against *G. mellonella* up to wt recipient strain levels. Survival curves are for *G. mellonella* larvae infected with the strains indicated. Larvae were injected with approximately 7.5×10^4 bacteria and incubated at 30°C in the dark. Live and dead larvae were counted at 24, 48, and 72 hpi. Curves represent the means of the results from three separate experiments, and error bars depict the standard deviation.

which encodes a regulator required for *afc* expression in *B. cenocepacia* K56-2 (24). H111 containing pC3del4, however, was found to have no antifungal activity against *F. solani*, suggesting that this cluster is either of lesser importance in H111, or that it is regulated by factors encoded elsewhere on pC3. In support of the first conclusion, an *afcA* mutant of H111 was unaffected in antifungal activity against *F. solani*, as was a *shvR* mutant (Fig. 3). Analysis of the partial pC3 derivatives showed that pC3del3 contains the region of pC3 that is most important for antifungal activity against both *R. solani* and *F. solani*, suggesting that this portion of pC3 either encodes an unknown antifungal agent or a regulator that controls the expression of an antifungal gene cluster located on one of the chromosomes.

Proteolytic activity is a known virulence factor, and proteases can degrade a range of host molecules, such as lactoferrin, type IV collagen, immunoglobulins, and antimicrobial peptides. The ZmpA protease, encoded on pC3, has been shown to be important in the rat agar bead model of infection but is not important in the *C. elegans* or *G. mellonella* models (21, 27, 29, 30). The derivative bearing the conserved part of pC3 did not confer proteolytic activity, while the nonconserved part of pC3, present on derivative pC3del2, conferred a level similar to that of the wild type. This derivative contains *zmpA*, as well as other putative protease-encoding genes (I35_7576, encoding a putative intracellular protease; I35_7645, encoding a putative Clp protease subunit; and I35_7805, encoding a putative serine protease). That proteolytic activity is encoded by the nonconserved part of H111 pC3 is consistent with previous findings that proteolytic activity is not a widespread pC3-dependent phenotype in the Bcc (9, 10). Analysis of the proteolytic activity exhibited by a conditional *zmpA* mutant showed that this gene is responsible for most, if not all, of the proteolytic activity associated with pC3. Interestingly, an *shvR* mutant of H111 showed wild-type levels of proteolytic activity in the azocasein assay and was unaffected in antifungal activity; these are both ShvR-regulated phenotypes in *B. cenocepacia* K56-2 (24), suggesting that ShvR is not involved in the regulation of proteolytic and antifungal activities in H111 (Fig. 3).

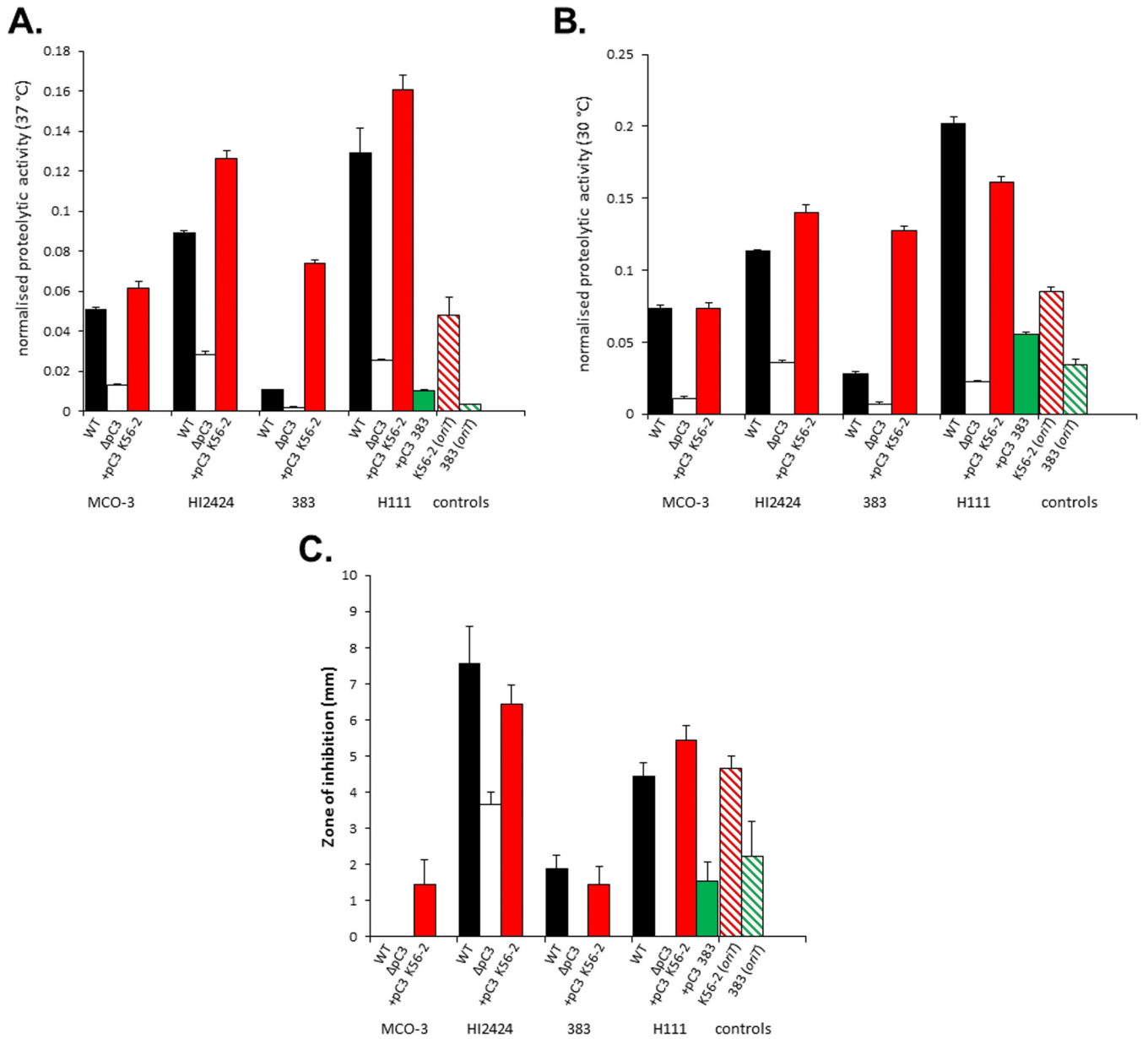


FIG 7 Phenotypes exhibited by strains bearing nonnative pC3s. For each set of bars, the strain background is given at the bottom of the graph (strains were *B. cenocepacia* MCO-3, HI2424, and H111 and *B. lata* 383). Black bars represent the value obtained for the wt, white bars are for the pC3-null derivative, and red bars are for the transfer strain bearing pC3_{K56-2}. For H111, a further transfer strain was constructed, bearing pC3₃₈₃, shown in green. Control strains were *B. cenocepacia* K56-2 and *B. lata* 383 bearing a mobilizable plasmid integrated into pC3 to allow transfer by conjugation. Error bars represent standard deviation across biological triplicates. (A) Proteolytic activity in cells grown at 37°C. Bars represent the normalized proteolytic activity of each strain. (B) Proteolytic activity in cells grown at 30°C. Bars represent the normalized proteolytic activity of each strain. (C) Antifungal activity against *F. solani*. Bars represent the mean zone of inhibition surrounding the bacteria. Plates were incubated at room temperature for 9 days.

Two animal models were used to assess the contribution of different parts of pC3 to H111 pathogenicity, those of *C. elegans* and *G. mellonella*. In *C. elegans*, the pC3del4 partial derivative conferred wild-type levels of virulence. This was probably due to the presence of *aidA* in this derivative. In *G. mellonella*, the conserved part of pC3 (pC3del1) conferred close-to-wild-type levels of virulence, but when this section was divided in two, one derivative showed only moderate virulence, and the other showed none. *AidA* is known not to affect virulence in the wax moth larva (22, 27). Three defined mutants of H111 were tested in the *G. mellonella* model: *afcA* and *shvR* deletion mutants and a *zmpA* conditional mutant. As would be expected, the *zmpA* conditional mutant showed virulence equal to that of its H111 parent strain, while both the *afcA* and *shvR* mutants

TABLE 1 Transfer of pC3 allows mingling of metabolic phenotypes between strains^a

Substrate ^b	H111	H111Δc3	H111/pC3 _{K56-2}	K56-2	K56-2Δc3	H111/pC3 ₃₈₃	383	383Δc3	Apparent source of phenotype
<i>N</i> -Acetyl D-glucosamine	+++	+++	+++	–	–	+++	–	–	H111 c1 or c2
Quinic acid	+++	+++	+++	–	–	+++	–	–	H111 c1 or c2
Tricarballic acid	–	–	+++	+++	–	–	–	–	K56-2 pC3
<i>m</i> -Tartaric acid	–	–	–	–	–	+++	+++	–	383 pC3

^aPhenotypic microarray analysis was used to analyze the indicated strains. In each case, the hybrid strain was compared with the wt parent and pC3 donor strains. +++, a ≥4-fold increase in OD₅₉₀; –, the OD₅₉₀ was equal to or lower than that of the negative control.

^bSubstrates shown gave rise to a difference in final OD₅₉₀ of >4×.

showed pathogenicity equal to that of H111Δc3 (Fig. 3). The ShvR regulator is necessary for expression of the *afcA* cluster in *B. cenocepacia* K56-2 (24), and these results suggest that *afcA* is an important virulence factor for the *G. mellonella* model. However, pC3del4 (carrying both *shvR* and the *afc* gene cluster) does not confer full virulence, suggesting that additional factors must be encoded by pC3, and that these are spread out in the conserved section rather than being in close proximity.

pC3 is a virulence plasmid, but the pathogenicity level of a Bcc strain is not entirely determined by its pC3. The *Burkholderia* strains used in this study exhibited similar levels of pathogenicity in the *G. mellonella* infection model but different levels of virulence in the *C. elegans* and zebrafish models.

Except for the pC3-deleted derivative of *B. lata* 383, which was not significantly less pathogenic than its wild-type parent in the *G. mellonella* model (Fig. 6), the deletion of pC3 reduced the virulence of all strains in all infection models, confirming a central role for pC3 in virulence (9, 10). To investigate whether virulence levels are entirely determined by the third replicon or are dependent on factors encoded by the two chromosomes, we exchanged pC3s between strains.

Transfer of pC3_{K56-2} restored virulence to H111, MCO-3, and HI2424 pC3-null strains in all models to approximately the level of the parent strain of the recipient. Using HI2424, however, which shows a reduced time to death compared to K56-2 only in zebrafish, we observed that pathogenicity to zebrafish was increased. Transfer of pC3₃₈₃ to H111 showed the same trend as the introduction of pC3_{K56-2} to this strain. In conclusion, the data presented in this study suggest that although pC3 is important for full virulence in all analyzed Bcc strains, chromosomally encoded factors determine the level of virulence that can be conferred by the addition of a heterologous pC3. The previous finding that in the absence of pC3 some (often quorum-sensing-regulated) genes on chromosomes 1 and 2 are not fully expressed (9) lends further support to this hypothesis.

Intriguingly, the proteolytic activities of the hybrid strains were often greater than those of both the recipient and the pC3 donor strain (Fig. 7A and B). The *zmpA* protease gene, present on both pC3₃₈₃ and pC3_{K56-2}, has been found to be regulated by various factors, including quorum sensing, AtsR (present on chromosome 2 in H111, HI2424, MCO-3, and 383), and ShvR (encoded on both pC3₃₈₃ and pC3_{K56-2}) (24, 31). Despite the sophisticated regulation of *zmpA*, we found that the transgenic strains possessed even higher levels of proteolytic activity than the parental strains, suggesting that the regulatory signatures of the incoming protease gene are readily recognized by the global regulatory circuitry.

Burkholderia spp. with antifungal activity have been used as biocontrol agents, for example, to protect against fungal diseases, such as damping off (32). Many Bcc members show potent antifungal activity, which has been found to be dependent on pC3 (9, 10). However, all Bcc members are currently excluded from use as biocontrol strains due to their status as opportunistic pathogens (<http://archive.epa.gov/scipoly/sap/meetings/web/pdf/finlrpt1.pdf>). We have shown here that antifungal activity can be transferred between *Burkholderia* species using pC3, whereas the virulence levels of hybrid strains depend on factors encoded by the chromosomes of the recipient strain. For example, transfer of pC3 from the epidemic and highly virulent strain *B. cenocepacia*

TABLE 2 Bacterial strains and plasmids used in this study

Strain or plasmid	Genotype or description ^a	Source or reference
Strains		
<i>B. cepacia</i> complex		
<i>B. lata</i> 383 (LMG 22485 ^T)	Soil isolate, prototroph	BCCM/LMG Bacteria Collection
<i>B. cenocepacia</i> H111	CF isolate, prototroph	46
<i>B. cenocepacia</i> MCO-3 (LMG 24308)	Soil isolate, prototroph	BCCM/LMG Bacteria Collection
<i>B. cenocepacia</i> H12424 (LMG 24507)	Soil isolate, prototroph	BCCM/LMG Bacteria Collection
<i>B. lata</i> 383Δc3	<i>B. lata</i> 383 (LMG 22485 ^T), c3 deletion mutant	9
<i>B. cenocepacia</i> H111Δc3	<i>B. cenocepacia</i> H111, c3 deletion mutant	9
<i>B. cenocepacia</i> MCO-3Δc3	<i>B. cenocepacia</i> MCO-3 (LMG 24308), c3 deletion mutant	9
<i>B. cenocepacia</i> H12424Δc3	<i>B. cenocepacia</i> H12424 (LMG 24507), c3 deletion mutant	9
<i>B. lata</i> 383Δc3/pC3 _{K56-2} Rif ^R	<i>B. lata</i> 383Δc3 rifampin-resistant mutant containing pC3 _{K56-2}	This study
<i>B. cenocepacia</i> H111Δc3/pC3 _{K56-2} Rif ^R	<i>B. cenocepacia</i> H111Δc3 rifampin-resistant mutant containing pC3 _{K56-2}	This study
<i>B. cenocepacia</i> MCO-3Δc3/pC3 _{K56-2} Rif ^R	<i>B. cenocepacia</i> MCO-3Δc3 rifampin-resistant mutant containing pC3 _{K56-2}	This study
<i>B. cenocepacia</i> H12424Δc3/pC3 _{K56-2} Rif ^R	<i>B. cenocepacia</i> H12424Δc3 rifampin-resistant mutant containing pC3 _{K56-2}	This study
<i>B. cenocepacia</i> H111Δc3/pC3 ₃₈₃ Rif ^R	<i>B. cenocepacia</i> H111Δc3 rifampin-resistant mutant containing pC3 ₃₈₃	This study
<i>B. cenocepacia</i> H111Δ <i>afcA</i>	<i>B. cenocepacia</i> H111 single-gene-deletion mutant of <i>afcA</i>	This study
<i>B. cenocepacia</i> H111- <i>shvR</i> ::Tp	<i>B. cenocepacia</i> H111 bearing a <i>dhfrIII</i> gene replacing the sequence between the Clal sites of <i>shvR</i>	This study
<i>B. cenocepacia</i> H111- <i>zmpA</i> ::pSC200	<i>B. cenocepacia</i> H111 conditional mutant, bearing pSC200 inserted into <i>zmpA</i>	This study
<i>E. coli</i> strains		
CC118(λpir)	Δ(<i>ara</i> , <i>leu</i>) ₇₆₉₇ <i>araD139</i> Δ <i>lacX74</i> <i>galE</i> <i>galk</i> <i>phoA20</i> <i>thi-1</i> <i>rpsE</i> <i>rpoB</i> (Rf ^r) <i>argE(am)</i> <i>recA1</i> λpir ⁺	39
MC1061	<i>hsdR</i> <i>araD139</i> Δ(<i>ara-leu</i>) ₇₆₉₇ Δ <i>lacX74</i> <i>galU</i> <i>galk</i> <i>rpsL</i> ; Sm ^r	47
Plasmids		
pSHAFT2	Broad-host-range suicide plasmid mobilizable for conjugation, Cm ^r	48
pBBR-5::FRT	pBBR1MCS-5 derivative encoding flippase	9
pRK2013	Helper plasmid for conjugation, ColE1 replicon, Km ^r	49
pEX18Tp	pEX18 containing <i>dhfrIII</i> between EcoRV and AatII sites, Tp ^r	9
pSHAFT2- <i>gabD</i>	pSHAFT2 bearing an amplified fragment of H111 pC3	10
pSHAFT2-FRT	Broad-host-range suicide plasmid mobilizable for conjugation, containing <i>FRT</i> site, Cm ^r	This study
pEX18Tp-FRT	pEX18 containing <i>dhfrIII</i> and <i>FRT</i> site, Tp ^r	This study
pSHAFT2-FRP	Broad-host-range suicide plasmid mobilizable for conjugation, Cm ^r , containing modified <i>FRT</i> site (FRP)	This study
pEX18Tp-FRP	pEX18 containing <i>dhfrIII</i> between EcoRV and AatII sites, containing modified <i>FRT</i> site (FRP), Tp ^r	This study

^aCF, cystic fibrosis; Rf^r, rifampin resistance; Sm^r, streptomycin resistance; Cm^r, chloramphenicol resistance; Km^r, kanamycin resistance; Tp^r, trimethoprim resistance.

K56-2 into the environmental Bcc isolate *B. lata* 383 resulted in a hybrid strain that exhibited a high level of antifungal activity but much lowered virulence in the *C. elegans* and zebrafish infection models relative to the *B. lata* 383 wild-type strain. Bacteria belonging to the Bcc are intracellular pathogens, as shown in *in vitro* cell culture studies and by using mammalian models, and this was recently confirmed in clinical studies (reference 33 and reviewed in reference 34). An intramacrophage stage has also been shown to be important for virulence of Bcc in zebrafish (35). Therefore, we will further exploit the advantages of noninvasive imaging in zebrafish embryos to determine the intracellular survival capacity and interaction of such hybrid strains with the host immune system. We are currently attempting to transfer pC3 from an antifungal Bcc strain into a strain of the environmental and beneficial *Burkholderia* clade (36, 37), with the aim of constructing a nonpathogenic hybrid with favorable properties for biocontrol. This could provide an important means of nonchemical control of fungus-borne diseases of plant crops.

MATERIALS AND METHODS

Bacterial strains and media. The bacterial strains used in this study are shown in Table 2. *Escherichia coli* and Bcc strains were routinely cultured at 37°C on LB Lennox agar containing antibiotics as appropriate, although the Iso-Sensitest (Oxoid) was used when the selective antibiotic was trimethoprim.

TABLE 3 Cloning details for construction of pC3 partial deletions

Partial derivative	Primer pair used ^a	Plasmid backbone	Restriction sites used ^b	Resultant plasmid
pC3del1	C3Up1StuFor, C3Up1XhoRev C3down1BamFor2, C3down1KpnRev2	pSHAFT2-FRT pEX18Tp-FRT	StuI and XhoI BamHI and KpnI	pSHAFT2-FRTc3Up pEX18Tp-FRTc3Down
pC3del2	pShaft2fwd1, pSHAFT2rev1 pEXfwd2, pEXrev2 pSHAFT2fwd3, pSHAFT2rev3 pEXfwd4, pEXrev4	pSHAFT2-FRT pEX18Tp-FRT pSHAFT2-FRP pEX18Tp-FRP	StuI and XhoI BamHI and EcoRI StuI and XhoI BamHI and EcoRI	pSHAFT2-FRT-hom1 pEX18Tp-FRT-hom2 pSHAFT2-FRP-hom3 pEX18Tp-FRP-hom4
pC3del3	pShaft2fwd1, pSHAFT2rev1 C3down1BamFor2, C3down1KpnRev2	pSHAFT2-FRT pEX18Tp-FRT	StuI and XhoI BamHI and KpnI	pSHAFT2-FRT-hom1 pEX18Tp-FRTc3Down
pC3del4	pEXfwd2, pEXrev2 pSHAFT2fwd3, pSHAFT2rev3 Hom5BamF, Hom5EcoR	pEX18Tp-FRT pSHAFT2-FRP pEX18Tp-FRP	BamHI and EcoRI StuI and XhoI BamHI and EcoRI	pEX18Tp-FRT-hom2 pSHAFT2-FRP-hom3 pEX18Tp-FRP-hom5

^aPCR amplification was carried out with the primer pairs given, using a boiled lysate of H111 colonies as the template. See Table 4 for primer sequences.

^bThe restriction sites given were used to cut the amplified DNA fragment and the backbone plasmid, and these were ligated and transformed as detailed in Materials and Methods.

The antibiotic concentrations used were as follows: chloramphenicol, 25 $\mu\text{g} \cdot \text{ml}^{-1}$ (*E. coli*) and 50 $\mu\text{g} \cdot \text{ml}^{-1}$ (Bcc); trimethoprim, 25 $\mu\text{g} \cdot \text{ml}^{-1}$ (*E. coli*) and 50 $\mu\text{g} \cdot \text{ml}^{-1}$ (Bcc); gentamicin, 20 $\mu\text{g} \cdot \text{ml}^{-1}$ (*E. coli* and Bcc); and rifampin, 50 $\mu\text{g} \cdot \text{ml}^{-1}$ (Bcc). M9 medium containing uracil as the nitrogen source, as described previously (9), was used for differentiation between wild-type and pC3-null Bcc strains.

Rifampin-resistant derivatives of strains were isolated by spreading 100 μl of a dense overnight culture on LB agar supplemented with rifampin (100 $\mu\text{g} \cdot \text{ml}^{-1}$) and incubated at 37°C until colonies appeared (approximately 3 days). Resistant colonies were purified by restreaking on LB agar supplemented with rifampin (50 $\mu\text{g} \cdot \text{ml}^{-1}$). No difference was observed in virulence in the different models between the rifampin-sensitive and rifampin-resistant versions of the different strains.

Molecular techniques. The plasmids used in this study are given in Table 2. Plasmid preparation was routinely carried out using the Qiagen miniprep kit. DNA prepared by PCR amplification or restriction digestion was purified using the Qiagen PCR purification kit. Molecular methods were carried out as described by Sambrook et al. (38).

Conjugal transfer of plasmids. Bacterial conjugations were used to introduce plasmids into Bcc strains, using a filter mating technique (39). A helper strain (MM294/pRK2013) was used to provide the *tra* genes. Conjugations were carried out on LB plates for approximately 16 h using saturated overnight cultures. *Pseudomonas* Isolation agar (PIA; Difco/Oxoid), supplemented with antibiotics as appropriate, was used for selection.

Construction of vectors for deletion of large genomic regions. Two pairs of plasmids were constructed to allow the directed deletion of two genomic regions from within the same strain. One pair contained an *FRT* site with the sequence gaagttcctattcTCTAGAAAgtaggaacttc (designated FRT), and the second pair contained a site with the sequence gaagttcctattcTCAAAATAgtaggaacttc (designated FRP). These sites consist of two binding regions (shown in lowercase in the two sequences above), separated by a spacer region (shown in uppercase in all FRT sequences). Flippase catalyzes recombination between sites with identical spacer regions, leaving an *FRT* site behind (40). This “scar” can be used for future rounds of recombination. Each plasmid pair consisted of a pSHAFT2 and a pEX18Tp derivative. Oligonucleotide pairs bearing the *FRT* sites were ordered from Microsynth and were as follows: pair 1 (for integrating FRT into pSHAFT2), FRTshaftNotEcoFor (ggccgcgaagttcctattcTCTAGAAAgtaggaacttcg) and FRTshaftNotEcoRev (aattcgaagttcctatacTTCTAGAGaataaggaacttcg); pair 2 (for integrating FRT into pEX18Tp), FRTpEXHindPstFor (agcttgaagttcctattcTCTAGAAAgtaggaacttcctgca) and FRTpEXHindPstRev (ggaagttcctatacTTCTAGAGaataaggaacttc); pair 3 (for integrating FRP into pSHAFT2), FRPshaftNotEcoFor (ggccgcgaagttcctattcTCAAAATAgtaggaacttcg) and FRPshaftNotEcoRev (aattcgaagttcctatacTATTGAAg aataggaacttcg); pair 4 (for integrating FRP into pEX18Tp), FRPpEXHindPstFor (agcttgaagttcctattcTCA AATAgtaggaacttcctgca) and FRPpEXHindPstRev (ggaagttcctatacTATTGAAg aataggaacttc). The oligonucleotide pairs were mixed (4,500 pmol each oligonucleotide) and heated to 90°C for 10 min in annealing buffer (final concentrations, 1 mM MgCl₂, 20 mM Tris-HCl [pH 8]). The reaction mixtures were allowed to cool at room temperature for 1 h to allow annealing of the pairs. The resultant double-stranded fragments were ligated directly into pSHAFT2/pEX18Tp digested with NotI and EcoRI/HindIII and PstI, respectively, to give vectors pSHAFT2-FRT, pEX18Tp-FRT, pSHAFT2-FRP, and pEX18Tp-FRP.

Tables 3 and 4 detail the primers used for the amplification of DNA homologous to the target regions and the restriction sites used for the insertion of these fragments into the empty vectors. Partial pC3 derivatives were constructed as follows: for pC3del1, pSHAFT2-FRTc3Up and pEX18Tp-FRTc3Down were introduced into H111 by conjugation, and correct integration by single homologous recombination was confirmed by PCR. Flippase-mediated excision of the DNA between the *FRT* sites was carried out by introduction of pBBR5::FLP, as previously described (9). pBBR5::FLP contains the *sacB* gene, which was used after each flippase recombination step to cure the strain of the plasmid. For pC3del2, pSHAFT2-FRT-hom1 and pEX18Tp-FRT-hom2 were introduced into H111, and correct integration by single homologous recombination was confirmed by PCR. pBBR5::FLP was introduced, and the DNA between

TABLE 4 Primers used for construction of pC3 partial deletions

Primer name	Primer sequence ^a
C3Up1StuFor	GCGCaggcctTTCCTCCCACGTATTACAGG
C3Up1XhoRev	GCGCctcgagTTCTACACGCATCACTTCG
C3down1BamFor2	GCGCggatccTCTGCTCTTGCTTTTTCCCC
C3down1KpnRev2	GCGCggatccCGGAATGAAGGGGAACATAG
pSHAFT2fwd1	GCGCaggcctCGCGACAAGACGCTTGAGTT
pSHAFT2rev1	GCGCctcgagAGTGC GGAGAGAATTGGGCG
pEXfwd2	GCGCggatccCTCACGCTCGAGCATTCTA
pEXrev2	GCGCgaattcTCAAAAAGAGAGTTTCAGCG
pSHAFT2fwd3	GCGCaggcctCAATCAATAACTCGCCACGA
pSHAFT2rev3	GCGCctcgagAACTTGAGCTTTCACCGACG
pEXfwd4	GCGCggatccCCGCGTCGCTGCACAGGAAC
pEXrev4	GCGCgaattcCGCAAAGCTGCTCGACGAAAC
Hom5BamF	GCGCggatccTCGAAAGGCGAGCTCGAGGC
Hom5EcoR	GCGCgaattcGCCAGCGCGGTCGACTTGAC

^aRestriction enzyme binding sites are shown in lowercase.

the FRT sites was excised. Plasmids pSHAFT2-FRP-hom3 and pEX18Tp-FRP-hom4 were then introduced and the correct integration confirmed, and pBBR5::FLP was used to excise the region between the FRP sites, leaving the desired section of pC3 and the pC3 origin of replication (see Fig. 1). For pC3del3, plasmids pSHAFT2-FRT-hom1 and pEX18Tp-FRTc3Down were introduced into H111 and the correct integration confirmed, and pBBR5::FLP was used to excise the region between the FRP sites. For pC3del4, plasmid pEX18Tp-FRT-hom2 was introduced into H111-pC3del1, and pBBR5::FLP was introduced, causing recombination between the FRT scar remaining within H111-pC3del1 and the FRT site from pEX18Tp-FRT-hom2. Plasmids pSHAFT2-FRP-hom3 and pEX18Tp-FRP-hom5 were then introduced and the correct integration confirmed, and pBBR5::FLP was used to excise the region between the FRP sites, leaving the desired section of pC3 and the pC3 origin of replication (see Fig. 1). The regions present on each derivative (relative to pC3_{H111}, accession number [NZ_HG938372](#)) were as follows; pC3del1, nucleotides (nt) 956415 to 1039263 and nt 1 to 367455; pC3del2, nt 366332 to 957407, and the origin of replication, nt 1036097 to 1039263 and nt 1 to 5738; pC3del3, nt 956415 to 1039263 and nt 1 to 20610; pC3del4, nt 956415 to 1039263 and nt 1 to 367455, and the origin of replication, nt 1036097 to 1039263 and nt 1 to 5738. All constructs were confirmed by amplification of the regions flanking the FRT scars, followed by sequencing. The following primer pairs were used for these purposes: to check pC3del1, Del4checkF (TAGATGTGCTCGTAGAG) and Del3checkR (AAGAGTCAGATGGAGTT GTA); to check pC3del2, Del2checkF (GGTCATCTGGTCTTGAATGG) and Del2checkR (GTGATGGACGA GATGACGC); to check pC3del3, Del3checkF (TGCCTATATCCTCGTGTTC) and Del3checkR; and to check pC3del4, Del4checkF and Del4checkR (GCGACGAAGAACAAGTA).

Construction of targeted mutants. *B. cenocepacia* strain H111-*shvR::dhfr* was constructed as follows: an ~2.2-kb region including *shvR* was amplified using primers *shvR*KpnF (GCGCGGTACCCCCGCATCAA GCAGATCTA) and *shvR*XbaR (GCGCTCTAGAGATCGAGTAATGCAGGGTA). This was digested and cloned into the KpnI and XbaI sites of pSHAFT2. The resultant plasmid was digested with ClaI, resulting in the excision of the majority of *shvR*. A *dhfrIII* trimethoprim resistance marker, amplified using primers *dhfr*claf (ggggatcgatcagttgacataagcctgttc) and *dhfr*clar (ggggatcgattagccacagtcagtgtg), was inserted into the ClaI-digested plasmid. This vector was transferred to H111 by conjugation. Double-crossover recombinants were selected using trimethoprim and subsequently screened for susceptibility to chloramphenicol. Correct replacement of the *shvR* fragment with *dhfrIII* was determined by PCR amplification and sequencing.

B. cenocepacia strain H111Δ*afcA* was constructed as follows: pSHAFT2-FRT-*afcUP* was constructed by amplifying an ~1,100-bp fragment of H111 pC3 using primers *afcUpF* (GGGGCTCGAGGATAGTTGTTGC CGTTCGTGA) and *afcUpR* (GGGGAGATCTTTACAGGCGGTAATGGTGAA), digested with XhoI and BglII, and inserted into these sites within pSHAFT2-FRT. This plasmid was transferred into H111 by conjugation, and single-crossover insertion mutants were selected on PIA supplemented with chloramphenicol and verified by sequencing across the joins between pC3 and the pSHAFT2-FRT-*afcUP*. pEX18Tp-FRT-DOWN was constructed by amplification of an ~1,200-bp fragment of H111 pC3 using primers *afcDownF* (GGGGGATCCAGGATCTGTGTTTCGTCGAG) and *afcDownR* (GGGGGAATTCATAGTCGAAGAAGCCGGG), digestion of this fragment with BamHI and EcoRI, and insertion into pEX18Tp-FRT digested with the same enzymes. This vector was transferred to H111 bearing the single-crossover insertion of pSHAFT2-FRT-*afcUP*, and insertion mutants were selected on PIA containing trimethoprim. Correct insertion was verified by PCR across the pC3-pEX18Tp-FRT-DOWN joins. Excision of *afcA* was achieved by the introduction of pBBR5::FLP, as described above.

B. cenocepacia strain H111-*zmpA::pSC200* was constructed as follows: an ~340-bp fragment of the H111 *zmpA* gene was amplified using primers *zmpA*condNdeF (GCGCCATATGAAGAACTGTCTCGA) and *zmpA*condXbaR (GCGCTCTAGACTTGCTCGAATGGACGAC), digested with NdeI and XbaI, and inserted into these sites within plasmid pSC200. This was transferred to H111 by conjugation, and single-crossover insertion mutants were selected on PIA plates containing trimethoprim. Correct insertion was verified by PCR amplification across the pC3-pSC200 joins. In the constructed mutant, *zmpA* was placed under the control of a rhamnose-inducible promoter, resulting in minimal expression in the absence of rhamnose.

pC3 transfers. For the transfer of *B. cenocepacia* K56-2 pC3, the K56-2-pC3::*gabD* mutant described by Agnoli et al. (10) was used as the donor. This mutant bears pSHAFT2 integrated into its pC3 and hence carries the pSHAFT2 *oriT* within this megaplasmid, enabling conjugative transfer of the replicon. Conjugal transfer and selection of exconjugants were also performed as described by Agnoli et al. (10).

For the transfer of *B. lata* 383 pC3, a fragment was amplified from *B. lata* 383 pC3 using primers araJXbaFor (GCGCTCTAGACGGTGTCTGGTCGATTTC) and araJBglRev (GCGCAGATCTGTACAGCCCGGAGA AAATC). The fragment was digested with XbaI and BglII and cloned into these sites within pSHAFT2 to produce pSHAFT2-*araJ*. This plasmid was integrated into pC3₃₈₃ by conjugation, resulting in the incorporation of an *oriT* within this replicon. Conjugal transfer was carried out as for the K56-2 pC3 transfers, and primers used for the differentiation of donor and recipient were cblCFor and cblCRev, and R33 For and R33Rev, with repAFor and repARev used for the detection of pC3 (see reference 10 for sequences).

Proteolytic activity assay. Proteolytic activity was assayed using cells grown at both 30°C and 37°C, based on the quantitative colorimetric method of Safarik (41), with modifications as described by Schmid and colleagues (42).

Antifungal activity assay. Fungus was prepared by transferring a plug of fungus into the center of a malt agar plate, sealing the plate with Parafilm, and incubating at room temperature in the dark for ~9 days for *Fusarium solani*, until the leading edge of the fungus neared the edge of the plate. Bacteria were cultured overnight in LB. Malt agar plates containing 2% agar were each inoculated with three 20- μ l spots of bacterial suspension, at points equidistant from the center of the plate. Plates were incubated at 37°C for 24 h. Fungal plugs were transferred from the youngest edge of the mycelium to the center of the plates and incubated at room temperature in the dark until a control fungal mycelium neared the edge of the plate. The assay was carried out in triplicate for each strain tested.

Pathogenicity assay using zebrafish embryos. The zebrafish embryo, with its innate immune system which resembles that of humans, has been well established as a model for Bcc virulence (35, 43). Depending on the bacterial strain, intravenously injected bacteria are rapidly phagocytosed by macrophages, culminating in disseminated proinflammatory lethal infection (as shown, for instance, for *B. cenocepacia* K56-2), or resulting in persistent infection with bacteria residing in macrophages (35). Since infection with H111 showed large variations in embryo survival between experiments, this strain was not analyzed using zebrafish in this study.

B. lata 383 and *B. cenocepacia* HI2424 and MCO-3 strains were analyzed for virulence in the zebrafish (*Danio rerio*) embryo model, as described previously (35, 43). Zebrafish (*Danio rerio*) were kept and handled in compliance with the guidelines of the European Union for handling laboratory animals (http://ec.europa.eu/environment/chemicals/lab_animals/home_en.htm). Zebrafish studies performed at U1047 are approved by the Direction Départementale de la Protection des Populations (DDPP) du Gard (ID 30-189-4) and the Comité d'Éthique pour l'Expérimentation Animale Languedoc-Roussillon (CEEA-LR-12186). Infection experiments were terminated before the larvae reached the free-feeding stage and did not classify as animal experiments according to the 2010/63/EU Directive (44).

Embryos were microinjected with the different strains, and the inoculum (CFU) was determined by injecting the same volume into a drop of phosphate-buffered saline (PBS) on LB agar ($n = 3$). For survival assays, embryos ($n = 20$ per strain per experiment) were individually kept in 48-well plates and analyzed at regular time intervals for mortality (scored by the absence of heartbeat). Experiments were performed at least three times, and the results from representative experiments are shown. Survival data are presented in Kaplan-Meier plots, and the significance of the data was analyzed with a log rank (Mantel-Cox) test.

Pathogenicity assay using *C. elegans* N2. Analysis of toxicity from bacterial strains toward *C. elegans* N2 was performed as previously described (45). Briefly, in a 96-well plate, 20 to 30 L1 larvae of *C. elegans* N2 were mixed with 80 μ l of bacterial culture adjusted to an optical density at 600 nm (OD_{600}) of 2.0. The plate was incubated for 48 h at 20°C. The developmental stage of the worms was determined. The data shown are means of at least 2 biological replicates.

Pathogenicity assay using *Galleria mellonella*. Infection of *G. mellonella* larvae was performed essentially as described previously (27). Briefly, *G. mellonella* organisms in the final larval stage (purchased from Fischerei Hebeisen, Zürich, or BioSystems Technology, UK) were stored at 10°C and used within 1 week. Bacterial cultures (grown overnight in LB at 37°C) were diluted 1:100 in 25 ml of LB broth and incubated with shaking at 30°C to an OD_{600} of 0.4 to 0.7. The bacteria were harvested and the pellets resuspended in 10 mM $MgSO_4$ (Merck). The OD_{600} was adjusted to 0.025, corresponding to $\sim 8 \times 10^6$ CFU \cdot ml⁻¹. For each assay, dilutions of the working solution were plated on LB to confirm the approximate initial dose. Ten-microliter aliquots were injected into the *G. mellonella* larvae via the hindmost proleg using a 10- μ l syringe (Hamilton) with a 27-gauge by 7/8 in. needle (Rose GmbH). For the negative-control larvae, 10 μ l of $MgSO_4$ was injected. To avoid contamination, the injection area was disinfected before inoculation using 70% ethanol. Ten randomly chosen larvae were used per strain tested, and each experiment was carried out in triplicate. The infected animals were incubated in petri dishes at 30°C in the dark. The number of dead larvae was counted at 24, 48, and 72 hpi. Larvae were considered dead when they did not respond to physical manipulation.

Phenotypic microarrays. Phenotypic microarrays were carried out using Biolog PM plates (PM1, 2a, and 3b). These test the range of carbon and nitrogen sources utilized by a bacterial strain. The assays were carried out according to the protocol supplied by the manufacturer. Glycerol stocks of bacterial strains were grown on R2A agar and passaged once on the same medium before testing. Cells were resuspended from R2A agar plates in Biolog inoculating fluid for analysis. Biolog microtiter plates were incubated at 37°C for 24 h. The OD_{590} of each well was determined using a plate reader (Bio-tek). The

criteria used to determine whether a phenotype differed between two strains were at least 50% difference between the OD₅₉₀ values for a given phenotype, with the higher value being at least 0.3. Where both strains being compared gave rise to OD₅₉₀ values of >1 for a given phenotype, no difference was scored. Each phenotypic difference was checked visually.

ACKNOWLEDGMENTS

We thank I. Scholl and C. Fabbri for superb technical assistance.

Financial support from the Swiss National Science Foundation (project 3100A0-104215) is gratefully acknowledged. A.C.V. was supported by a grant from the Marie Curie Initial Training Network FishForPharma (PITN-GA-2011-289209). M.C.G. was recipient of a doctoral grant from the French Ministry of Higher Education and Research (MENSUR).

REFERENCES

- Drevinek P, Mahenthalingam E. 2010. *Burkholderia cenocepacia* in cystic fibrosis: epidemiology and molecular mechanisms of virulence. *Clin Microbiol Infect* 16:821–830. <https://doi.org/10.1111/j.1469-0691.2010.03237.x>.
- Peeters C, Zlosnik JE, Spilker T, Hird TJ, LiPuma JJ, Vandamme P. 2013. *Burkholderia pseudomultivorans* sp. nov., a novel *Burkholderia cepacia* complex species from human respiratory samples and the rhizosphere. *Syst Appl Microbiol* 36:483–489. <https://doi.org/10.1016/j.syapm.2013.06.003>.
- De Smet B, Mayo M, Peeters C, Zlosnik JE, Spilker T, Hird TJ, LiPuma JJ, Kidd TJ, Kaestli M, Ginther JL, Wagner DM, Keim P, Bell SC, Jacobs JA, Currie BJ, Vandamme P. 2015. *Burkholderia stagnalis* sp. nov. and *Burkholderia territorii* sp. nov., two novel *Burkholderia cepacia* complex species from environmental and human sources. *Int J Syst Evol Microbiol* 65:2265–2271. <https://doi.org/10.1099/ijss.0.000251>.
- Ong KS, Aw YK, Lee LH, Yule CM, Cheow YL, Lee SM. 2016. *Burkholderia paludis* sp. nov., an antibiotic-siderophore-producing novel *Burkholderia cepacia* complex species, isolated from Malaysian tropical peat swamp soil. *Front Microbiol* 7:2046. <https://doi.org/10.3389/fmicb.2016.02046>.
- Li GX, Wu XQ, Ye JR. 2013. Biosafety and colonization of *Burkholderia multivorans* WS-FJ9 and its growth-promoting effects on poplars. *Appl Microbiol Biotechnol* 97:10489–10498. <https://doi.org/10.1007/s00253-013-5276-0>.
- Baldwin A, Mahenthalingam E, Drevinek P, Vandamme P, Govan JR, Waine DJ, LiPuma JJ, Chiarini L, Dalmastris C, Henry DA, Speert DP, Honeybourne D, Maiden MCJ, Dowson CG. 2007. Environmental *Burkholderia cepacia* complex isolates in human infections. *Emerg Infect Dis* 13:458–461. <https://doi.org/10.3201/eid1303.060403>.
- LiPuma JJ, Spilker T, Coenye T, Gonzalez CF. 2002. An epidemic *Burkholderia cepacia* complex strain identified in soil. *Lancet* 359:2002–2003. [https://doi.org/10.1016/S0140-6736\(02\)08836-0](https://doi.org/10.1016/S0140-6736(02)08836-0).
- Eberl L, Vandamme P. 2016. Members of the genus *Burkholderia*: good and bad guys. *F1000Res*. 5:F1000 Faculty Rev-1007. <https://doi.org/10.12688/f1000research.8221.1>.
- Agnoli K, Schwager S, Uehlinger S, Vergunst A, Viteri DF, Nguyen DT, Sokol PA, Carlier A, Eberl L. 2012. Exposing the third chromosome of *Burkholderia cepacia* complex strains as a virulence plasmid. *Mol Microbiol* 83:362–378. <https://doi.org/10.1111/j.1365-2958.2011.07937.x>.
- Agnoli K, Frauenknecht C, Freitag R, Schwager S, Jenul C, Vergunst A, Carlier A, Eberl L. 2014. The third replicon of members of the *Burkholderia cepacia* complex, plasmid pC3, plays a role in stress tolerance. *Appl Environ Microbiol* 80:1340–1348. <https://doi.org/10.1128/AEM.03330-13>.
- Chain PS, Deneff VJ, Konstantinidis KT, Vergez LM, Agullo L, Reyes VL, Hauser L, Cordova M, Gomez L, Gonzalez M, Land M, Lao V, Larimer F, LiPuma JJ, Mahenthalingam E, Malfatti SA, Marx CJ, Parnell JJ, Ramette A, Richardson P, Seeger M, Smith D, Spilker T, Sul WJ, Tsoi TV, Ulrich LE, Zhulin IB, Tiedje JM. 2006. *Burkholderia xenovorans* LB400 harbors a multi-replicon, 9.73-Mbp genome shaped for versatility. *Proc Natl Acad Sci U S A* 103:15280–15287. <https://doi.org/10.1073/pnas.0606924103>.
- Reyes-Gallegos RI, Ramirez-Diaz MI, Cervantes C. 2016. *chr* genes from adaptive replicons are responsible for chromate resistance by *Burkholderia xenovorans* LB400. *World J Microbiol Biotechnol* 32:45. <https://doi.org/10.1007/s11274-015-1996-x>.
- diCenzo GC, Checucci A, Bazzicalupo M, Mengoni A, Viti C, Dziewit L, Finan TM, Galardini M, Fondi M. 2016. Metabolic modelling reveals the specialization of secondary replicons for niche adaptation in *Sinorhizobium meliloti*. *Nat Commun* 7:12219. <https://doi.org/10.1038/ncomms12219>.
- Juhas M, Stark M, von Mering C, Lumjaktase P, Crook DW, Valvano MA, Eberl L. 2012. High confidence prediction of essential genes in *Burkholderia cenocepacia*. *PLoS One* 7:e40064. <https://doi.org/10.1371/journal.pone.0040064>.
- Galardini M, Pini F, Bazzicalupo M, Biondi EG, Mengoni A. 2013. Replicon-dependent bacterial genome evolution: the case of *Sinorhizobium meliloti*. *Genome Biol Evol* 5:542–558. <https://doi.org/10.1093/gbe/evt027>.
- Lu SE, Novak J, Austin FW, Gu G, Ellis D, Kirk M, Wilson-Stanford S, Tonelli M, Smith L. 2009. Occidiofungin, a unique antifungal glycopeptide produced by a strain of *Burkholderia contaminans*. *Biochemistry* 48:8312–8321. <https://doi.org/10.1021/bi900814c>.
- Moon SS, Kang PM, Park KS, Kim CH. 1996. Plant growth promoting and fungicidal 4-quinolinones from *Pseudomonas cepacia*. *Phytochemistry* 42:365–368. [https://doi.org/10.1016/0031-9422\(95\)00897-7](https://doi.org/10.1016/0031-9422(95)00897-7).
- Vial L, Lepine F, Milot S, Groleau MC, Dekimpe V, Woods DE, Deziel E. 2008. *Burkholderia pseudomallei*, *B. thailandensis*, and *B. ambifaria* produce 4-hydroxy-2-alkylquinoline analogues with a methyl group at the 3 position that is required for quorum-sensing regulation. *J Bacteriol* 190:5339–5352. <https://doi.org/10.1128/JB.00400-08>.
- Mahenthalingam E, Song LJ, Sass A, White J, Wilmot C, Marchbank A, Boaisa O, Paine J, Knight D, Challis GL. 2011. Enacyloxins are products of an unusual hybrid modular polyketide synthase encoded by a cryptic *Burkholderia ambifaria* genomic island. *Chem Biol* 18:665–677. <https://doi.org/10.1016/j.chembiol.2011.01.020>.
- Kang YW, Carlson R, Tharpe W, Schell MA. 1998. Characterization of genes involved in biosynthesis of a novel antibiotic from *Burkholderia cepacia* BC11 and their role in biological control of *Rhizoctonia solani*. *Appl Environ Microbiol* 64:3939–3947.
- Corbett CR, Burntack MN, Kooi C, Woods DE, Sokol PA. 2003. An extracellular zinc metalloprotease gene of *Burkholderia cepacia*. *Microbiology* 149:2263–2271. <https://doi.org/10.1099/mic.0.26243-0>.
- Huber B, Feldmann F, Kothe M, Vandamme P, Wopperer J, Riedel K, Eberl L. 2004. Identification of a novel virulence factor in *Burkholderia cenocepacia* H111 required for efficient slow killing of *Caenorhabditis elegans*. *Infect Immun* 72:7220–7230. <https://doi.org/10.1128/IAI.72.12.7220-7230.2004>.
- Subramoni S, Nguyen DT, Sokol PA. 2011. *Burkholderia cenocepacia* ShvR-regulated genes that influence colony morphology, biofilm formation, and virulence. *Infect Immun* 79:2984–2997. <https://doi.org/10.1128/IAI.00170-11>.
- O'Grady EP, Nguyen DT, Weisskopf L, Eberl L, Sokol PA. 2011. The *Burkholderia cenocepacia* LysR-type transcriptional regulator ShvR influences expression of quorum-sensing, protease, type II secretion, and *afc* genes. *J Bacteriol* 193:163–176. <https://doi.org/10.1128/JB.00852-10>.
- Loutet SA, Valvano MA. 2010. A decade of *Burkholderia cenocepacia* virulence determinant research. *Infect Immun* 78:4088–4100. <https://doi.org/10.1128/IAI.00212-10>.
- Gingues S, Kooi C, Visser MB, Subsin B, Sokol PA. 2005. Distribution and expression of the ZmpA metalloprotease in the *Burkholderia cepacia* complex. *J Bacteriol* 187:8247–8255. <https://doi.org/10.1128/JB.187.24.8247-8255.2005>.
- Uehlinger S, Schwager S, Bernier SP, Riedel K, Nguyen DT, Sokol PA, Eberl L. 2009. Identification of specific and universal virulence factors in

- Burkholderia cenocepacia* strains by using multiple infection hosts. *Infect Immun* 77:4102–4110. <https://doi.org/10.1128/IAI.00398-09>.
28. Drevinek P, Baldwin A, Dowson CG, Mahenthiralingam E. 2008. Diversity of the *parB* and *repA* genes of the *Burkholderia cepacia* complex and their utility for rapid identification of *Burkholderia cenocepacia*. *BMC Microbiol* 8:44. <https://doi.org/10.1186/1471-2180-8-44>.
 29. Kooi C, Sokol PA. 2009. *Burkholderia cenocepacia* zinc metalloproteases influence resistance to antimicrobial peptides. *Microbiology* 155: 2818–2825. <https://doi.org/10.1099/mic.0.028969-0>.
 30. Bernier SP, Silo-Suh L, Woods DE, Ohman DE, Sokol PA. 2003. Comparative analysis of plant and animal models for characterization of *Burkholderia cepacia* virulence. *Infect Immun* 71:5306–5313. <https://doi.org/10.1128/IAI.71.9.5306-5313.2003>.
 31. Aubert DF, O'Grady EP, Hamad MA, Sokol PA, Valvano MA. 2013. The *Burkholderia cenocepacia* sensor kinase hybrid AtsR is a global regulator modulating quorum-sensing signalling. *Environ Microbiol* 15:372–385. <https://doi.org/10.1111/j.1462-2920.2012.02828.x>.
 32. Coenye T, Vandamme P. 2003. Diversity and significance of *Burkholderia* species occupying diverse ecological niches. *Environ Microbiol* 5:719–729. <https://doi.org/10.1046/j.1462-2920.2003.00471.x>.
 33. Schwab U, Abdullah LH, Perlmutter OS, Albert D, Davis CW, Arnold RR, Yankaskas JR, Gilligan P, Neubauer H, Randell SH, Boucher RC. 2014. Localization of *Burkholderia cepacia* complex bacteria in cystic fibrosis lungs and interactions with *Pseudomonas aeruginosa* in hypoxic mucus. *Infect Immun* 82:4729–4745. <https://doi.org/10.1128/IAI.01876-14>.
 34. Valvano MA. 2015. Intracellular survival of *Burkholderia cepacia* complex in phagocytic cells. *Can J Microbiol* 61:607–615. <https://doi.org/10.1139/cjm-2015-0316>.
 35. Vergunst AC, Meijer AH, Renshaw SA, O'Callaghan D. 2010. *Burkholderia cenocepacia* creates an intramacrophage replication niche in zebrafish embryos, followed by bacterial dissemination and establishment of systemic infection. *Infect Immun* 78:1495–1508. <https://doi.org/10.1128/IAI.00743-09>.
 36. Estrada-de los Santos P, Vinuesa P, Martinez-Aguilar L, Hirsch AM, Caballero-Mellado J. 2013. Phylogenetic analysis of *Burkholderia* species by multilocus sequence analysis. *Curr Microbiol* 67:51–60. <https://doi.org/10.1007/s00284-013-0330-9>.
 37. Suárez-Moreno ZR, Caballero-Mellado J, Coutinho BG, Mendonça-Previato L, James EK, Venturi V. 2012. Common features of environmental and potentially beneficial plant-associated *Burkholderia*. *Microb Ecol* 63:249–266. <https://doi.org/10.1007/s00248-011-9929-1>.
 38. Sambrook J, Fritsch EF, Maniatis T. 1989. *Molecular cloning: a laboratory manual*, 2nd ed. Cold Spring Harbor Laboratory Press, Cold Spring Harbor, NY.
 39. Herrero M, Delorenzo V, Timmis KN. 1990. Transposon vectors containing non-antibiotic resistance selection markers for cloning and stable chromosomal insertion of foreign genes in Gram-negative bacteria. *J Bacteriol* 172:6557–6567. <https://doi.org/10.1128/jb.172.11.6557-6567.1990>.
 40. Senecoff JF, Rossmessl PJ, Cox MM. 1988. DNA recognition by the FLP recombinase of the yeast 2 μ plasmid. A mutational analysis of the FLP binding site. *J Mol Biol* 201:405–421.
 41. Safarik I. 1987. Thermally modified azocasein—a new insoluble substrate for the determination of proteolytic activity. *Biotechnol Appl Biochem* 9:323–324.
 42. Schmid N, Pessi G, Deng Y, Aguilar C, Carlier AL, Grunau A, Omasits U, Zhang LH, Ahrens CH, Eberl L. 2012. The AHL- and BDSF-dependent quorum sensing systems control specific and overlapping sets of genes in *Burkholderia cenocepacia* H111. *PLoS One* 7:e49966. <https://doi.org/10.1371/journal.pone.0049966>.
 43. Mesureur J, Vergunst AC. 2014. Zebrafish embryos as a model to study bacterial virulence. *Methods Mol Biol* 1197:41–66. https://doi.org/10.1007/978-1-4939-1261-2_3.
 44. European Union. 2010. Directive 2010/63/EU of the European Parliament and of the Council of 22 September 2010 on the protection of animals used for scientific purposes. European Union, Brussels, Belgium. <http://eur-lex.europa.eu/legal-content/EN/TXT/?uri=CELEX:32010L0063>.
 45. Lardi M, Aguilar C, Pedrioli A, Omasits U, Suppiger A, Carcamo-Oyarce G, Schmid N, Ahrens CH, Eberl L, Pessi G. 2015. σ 54-dependent response to nitrogen limitation and virulence in *Burkholderia cenocepacia* strain H111. *Appl Environ Microbiol* 81:4077–4089. <https://doi.org/10.1128/AEM.00694-15>.
 46. Römmling U, Fiedler B, Bosshammer J, Grothues D, Greipel J, Vonderhardt H, Tummeler B. 1994. Epidemiology of chronic *Pseudomonas aeruginosa* infections in cystic fibrosis. *J Infect Dis* 170:1616–1621. <https://doi.org/10.1093/infdis/170.6.1616>.
 47. Casadaban MJ, Cohen SN. 1980. Analysis of gene control signals by DNA fusion and cloning in *Escherichia coli*. *J Mol Biol* 138:179–207. [https://doi.org/10.1016/0022-2836\(80\)90283-1](https://doi.org/10.1016/0022-2836(80)90283-1).
 48. Shastri S, Spiewak HL, Sofoluwe A, Eidsvaag VA, Asghar AH, Pereira T, Bull EH, Butt AT, Thomas MS. 2016. An efficient system for the generation of marked genetic mutants in members of the genus *Burkholderia*. *Plasmid* 89:49–56. <https://doi.org/10.1016/j.plasmid.2016.11.002>.
 49. Figurski DH, Helinski DR. 1979. Replication of an origin-containing derivative of plasmid Rk2 dependent on a plasmid function provided in *trans*. *Proc Natl Acad Sci U S A* 76:1648–1652. <https://doi.org/10.1073/pnas.76.4.1648>.